Int. J. Nano Dimens., 9 (2): 198-208, Spring 2018

ORIGINAL ARTICLE

Comparative account of antifungal activity of green and chemically synthesized Zinc Oxide nanoparticles in combination with agricultural fungicides

Pragati Jamdagni*; Jogender Singh Rana; Poonam Khatri; Kiran Nehra

Department of Biotechnology, Deenbandhu Chhotu Ram University of Science and Technology, Murthal- 131039, Sonipat, Haryana, India

Received 09 November 2017; revised 29 January 2018; accepted 03 February 2018; available online 08 February 2018

Abstract

The present study aims at study on combined effect of zinc oxide nanoparticles (ZnO) with common agricultural fungicides. Nanoparticles were synthesized using chemical reduction process and characterized through UV-Visible spectroscopy, X-ray diffraction (XRD), Dynamic Light Scattering (DLS) and Transmission Electron Microscopy (TEM). Synthesized nanoparticles were observed to be in size range of 12-63 nm as confirmed by TEM micrograph. DLS established polydisperse nature of nanoparticles and provided effective hydrodynamic diameter of 76.15 nm, confirming the hypothesis of particles being in nano range. Nanoparticles were tested against fungal phytopathogens, namely *A. alternata, A. niger, B. cinerea, F. oxysporum* and *P. expansum*. Nanoparticles used in the study exhibited good antifungal activity. Both classes of nanoparticles (green and chemically synthesized) were individually tested against fungal phytopathogens and in combination with fungicides. Nanoparticles positively influenced the inhibitory effects of fungicides. *P. expansum* was observed to be the most sensitive fungus. It exhibited sharp decrease in MIC values from 2 µg/mL for carbendazim and 4 µg/mL for thiram to 0.25 µg/mL when carbendazim and thiram were used in combination with green ZnO NPs. Mean MIC value (mean ± sd) for combination of all three fungicides with green ZnO NPs was 0.83 ± 0.4 µg/mL and for chemical ZnO NPs was 1.17 ± 0.7 µg/mL. Hence, green ZnO NPs showed better inhibition of test fungi when compared to chemically synthesized ZnO NPs. In summary, the study reports synthesis of ZnO nanoparticles with good antimicrobial potential and amelioration of activity of fungicides was observed when used in combination with nanoparticles.

Keywords: *Antifungal activity; Fungicides; Minimum inhibitory concentration (MIC); Nanoparticle synthesis; Zinc oxide.*

How to cite this article

Jamdagni P, Singh Rana J, Khatri P, NehraK. Comparative account of antifungal activity of green and chemically synthesized Zinc Oxide nanoparticles in combination with agricultural fungicides. Int. J. Nano Dimens., 2018; 9(2): 198-208.

INTRODUCTION

Plants are major food provider for humans all over the world and are imperative for human existence and survival. Apart from humans, a wide range of organisms and microorganism also maneuver plants as a source of food and shelter. During this process, some of these organisms cause diseases to their hosts which eventually lead to the depreciation of their yield and heavy economic losses. Of these, fungal diseases have been reported to cause major yield losses [1, 2]. As per recent reports, about 125 million tones of world's five most important crops, viz., rice, wheat, maize, potatoes and soybeans, are destroyed because of fungal infections every year, making it one of the major threats for global food security. This quantity is sufficient to feed approximately 600 million of the hungry population [3]. Even if the economic and yield losses are excluded, fungal pathogens, such as *Penicillium, Fusarium and Alternaria*, can pose severe health risks by means of mycotoxins released into the infected material [4]. Broad spectrum fungicides and soil fumigating biocides are being currently used to control and

* Corresponding Author Email: *pragati_318@yahoo.co.in*

combat fungal infection. But, with their continuous use the problem of fungicide resistance is now coming up, where fungal pathogens are becoming increasingly resistant to fungicides [5]. Hence, there is a need to find alternatives to these common fungicides.

Recent advances in nanotechnology hold promise for such alternatives. Several classes of nanostructures are being synthesized and find applications in various fields of life, most important being medicine, healthcare and as antimicrobials [6-17]. Zinc oxide nanoparticles (ZnO NPs), in particular, have a wide spectrum of applications to offer. ZnO has been, in general, recognized as safe (GRAS) material category by the US Food and Drug Administration [18] and ZnO NPs are finding increased applications in day-to-day lives with inclusion in products such as cosmetics ointments, food packaging etc. [19-22]. An important and well researched property associated with ZnO is their excellent photocatalytic activity [23-25]. Lately, ZnO nanostructures are being extensively researched for their antimicrobial activities and are found to be active against various microorganisms [26, 27].

The current study reports chemical synthesis of ZnO NPs and their antifungal potential. Further, these NPs, along with green synthesized ZnO NPs were used in combination with commonly used fungicides, namely, carbendazim (Methyl 2-benzimidazole carbamate), mancozeb (Manganese zinc ethylene bis (dithiocarbamate)) and thiram (bis (dimethyl thiocarbamoyl) disulfide). All three have been registered under section 9(3) of the Insecticides Act, 1968 for use in India [28]. Reports are available that indicate synergism between ZnO NPs and antibiotics but few concern the combined effects of these NPs with above stated fungicides. The results indicate a positive interaction between the two and inhibitory effect of fungicides appears to improve in the presence of nanoparticles.

EXPERIMENTAL

Materials

All the chemicals used for nanoparticle synthesis were obtained from Thermo Fisher Scientific India Pvt. Ltd. (Mumbai). Fungicides used were of analytical grade and procured from Sigma-Aldrich Chemicals Pvt. Ltd. (Bangalore). Fungal phytopathogens, namely *Alternaria alternata* (ITCC 6531), *Aspergillus niger* (ITCC 7122), *Botrytis cinerea* (ITCC 6192), *Fusarium oxysporum* (ITCC 55) and *Penicillium expansum* (ITCC 6755) were procured from Indian Type Culture Collection, Indian Agricultural Research Institute, New Delhi, India.

Synthesis of Zinc Oxide Nanoparticles

Green ZnO NPs were synthesized at optimized conditions using flower extract of *Nyctanthes arbor-tristis* as described previously [29]. 50 mL of 0.01M zinc acetate solution was taken to which 1 mL of flower extract was added. Under continuous stirring, pH of the mixture was increased to 12 with the help of 2M NaOH. The temperature of synthesis was maintained at 90°C and the mixture was stirred for 2 h. Pale white precipitate observed after 2 h was washed and dried at 90°C overnight. Chemical synthesis of ZnO NPs was performed with the help of sodium hydroxide as described by Gnanasangeetha and Thambavani [30] with minor modifications. Briefly, 50 mL of 0.02 M solution of zinc acetate was used as the precursor and 2 M NaOH was dropwise added to increase the pH of the solution to 12, heating the solution at the constant temperature of 90 °C. After continuous stirring for 2-3 h, the appearance of white precipitate was observed; this was washed twice with sterile de-ionized water and dried in hot air oven at 90 °C overnight. Complete conversion to ZnO nanoparticles takes place during drying.

Characterization of Chemical ZnO NPs

Chemically synthesized ZnO NPs were characterized using UV-Visible spectroscopy, X-ray diffraction, dynamic light scattering and transmission electron microscopy to ascertain their shape and size. Washed and dried ZnO nanopowder was re-suspended in sterile de-ionized water to yield a dilute suspension and UV-Visible spectrum was generated using UV-Vis Spectrophotometer UV-3092 from Labindia Analytical Instruments Pvt. Ltd., in the wavelength range of 200-700 nm with 1 nm resolution [31]. Distilled water was used to set the reference baseline before performing spectral measurement studies and spectra for zinc acetate dihydrate, sodium hydroxide and plant extract were noted to serve as negative controls. No peaks were observed in any of the three control suspensions.

For X-ray diffraction (XRD) studies, the nanopowder was analyzed using Ultima IV (Rigaku, Japan), with an X-ray wavelength of 1.5406 Å.

Diffraction data were recorded in the 2θ range of 20-70 degrees at tube voltage and current of 40 kV and 40 mA, respectively, in 2θ/θ continuous scanning mode [29].

Dynamic Light Scattering (DLS) was performed using Zetasizer Nano (DLS, Malvern Instruments, Worcestershire, UK), outfitted with a He/Ne red laser of wavelength 633 nm and a detector fixed at 173°. ZnO nanopowder was suspended in sterile de-ionized water and sonicated for 15 min prior to analysis and measurements were recorded as a function of time [32].

Transmission electron microscopy (TEM) was performed using Morgagni 268D, FEI Electron Optics (USA), at an accelerating voltage of 200 kV. ZnO nanopowder was again suspended in sterile deionized water, sonicated for 10 min and coated onto a copper grid for visualization [33].

Antifungal Activity

Chemically synthesized ZnO NPs were tested for antifungal potential against *Alternaria alternata*, *Aspergillus niger, Botrytis cinerea*, *Fusarium oxysporum* and *Penicillium expansum*. The minimum inhibitory concentration of ZnO NPs was calculated using broth dilution method. The initial concentration used was 256 µg/mL, which was diluted two fold in consecutively numbered tubes [29]. To study the effect of nanoparticles (green synthesized and chemically synthesized) on the efficacy of fungicides, nanoparticles and fungicides were mixed in equal concentrations (256 µg/mL each) and incubated overnight. These combinations were then used to determine MIC values against above stated phytopathogens. Fungicides used in the study were carbendazim, mancozeb and thiram. Six combinations were studied, namely, carbendazim with green ZnO NPs (CGZ) and chemical ZnO NPs (CCZ); mancozeb with green ZnO NPs (MGZ) and chemical ZnO NPs (MCZ) and thiram with green ZnO NPs (TGZ) and chemical ZnO NPs (TCZ). All the experiments were performed in triplicates.

Statistical Analysis

Results of combined tests were analyzed using paired sample t-test using Origin Pro 8 to determine if there was a statistically significant mean difference between the MIC values of individual fungicides (first set of observations) and fungicides combined with nanoparticles (second set of observations). Data obtained for CGZ and CCZ was compared with carbendazim, for MGZ and MCZ were compared with mancozeb and for TGZ and TCZ were compared with thiram for paired sample t-test.

RESULTS AND DISCUSSION

Synthesis and Characterization of ZnO Nanoparticles

Addition of NaOH to the parent solution of zinc acetate resulted in the formation of a white precipitate. This precipitate was washed and dried overnight to yield ZnO nanopowder (Fig. 1a). Proposed mechanism for reaction is as follows [34]:

$$Zn(CH_3COO)_2.2H_2O + 2NaOH \rightarrow ZnO + 2NaCH_3COO + H_2O$$

UV-Visible spectrum of chemically synthesized ZnO nanopowder was obtained upon re-suspension in sterile deionized water and a sharp absorption peak was observed at 362 nm (Fig. 1b). The nanopowder was transferred to sterile centrifuge tubes and stored in dried form.

TEM imaging (Fig. 2) of synthesized nanoparticles confirmed nanoscale dimensions of synthesized ZnO NPs and provided a particle size range of 12-40 nm. DLS analysis depicted an average particle size of 76.15 nm and the polydispersity index of 0.493 (Fig. 3). TEM images provide size measurement of the metallic core of individual particles, while the hydrodynamic diameter is calculated as the total size of the core particle and the shell or layer that envelops the core during reduction process [35]. Moreover, aggregation brings two or more particles in close association and can cause further variations in actual particle size and the average hydrodynamic diameter. TEM images confirm the presence of NPs in the form of aggregates validating their polydisperse nature, which is quite common for nanoparticles obtained in form of dried powder.

Fig. 4 shows a typical X-ray diffractogram for ZnO NPs in the 2θ range of 20-70°. XRD data was used for particle size calculations and determination of crystal lattice indices. Various peaks corresponding to Bragg's reflections were observed at 2θ values of 31.86°, 34.52°, 36.34°, 47.56°, 56.74°, 62.96°, 66.46°, 67.98° and 69.14° corresponding to (100), (002), (101), (102), (110), (103), (200), (112) and (201) lattice planes respectively. All these peaks were indexed as per the hexagonal phase of zinc oxide (JCPDS file: 36-1451) and found to be in accordance with previous reports [36-38]. The

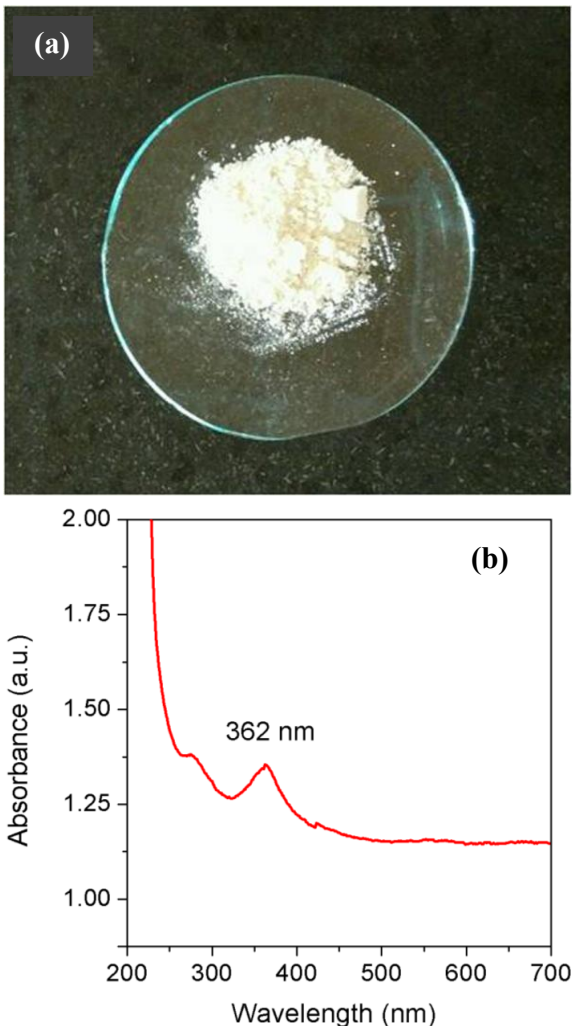

Fig. 1: a) Zinc oxide nanopowder obtained after overnight drying, b) UV-Visible spectrum of chemical ZnO NPs.

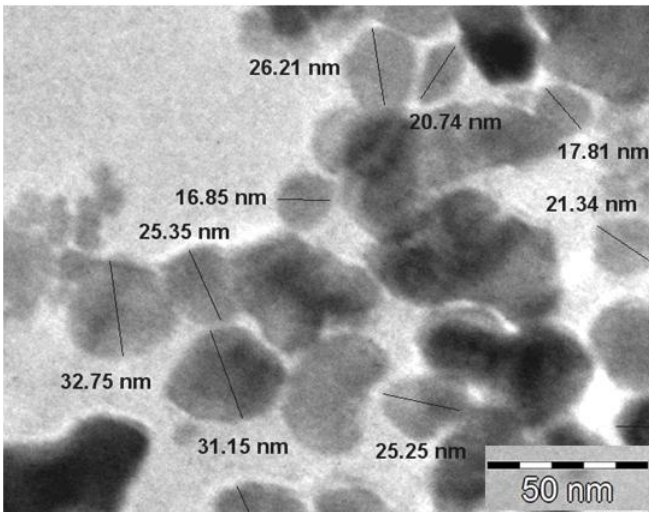

Fig. 2: TEM micrograph of ZnO NPs.

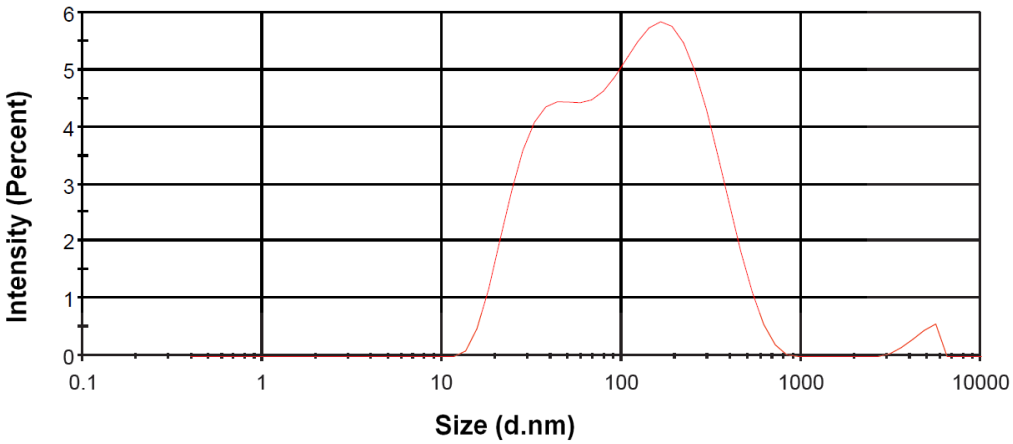

Fig. 3: DLS plot for ZnO NPs.

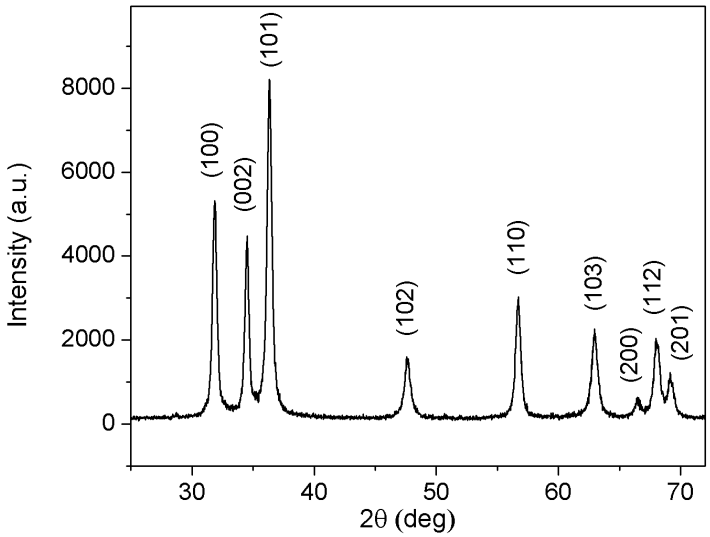

Fig. 4: X-ray diffractogram of chemically synthesized ZnO NPs.

absence of any accessory peaks confirms the purity and good crystalline state of synthesized nanoparticles.

Bragg's law equation was used to determine the interplanar *d*- spacing (Table 1):

$$2d\sin\theta = n\lambda$$

Where, *d* is the interplanar spacing, θ is Bragg's angle of diffraction, *n* = 1 and λ is wavelength of X-ray used (1.5406 Å).

Debye–Scherrer equation was used to calculate average particle size from the dominant peak at 36.34°, corresponding to (101) plane [36],

$$D = 0.89\lambda / \beta\cos\theta$$

Where, *D* is the average particle size, 0.89 is the Scherrer's constant, λ is X-ray (1.5406 Å) and β is FWHM (Full Width at Half Maximum) of the dominant (101) peak and θ is Bragg's angle of diffraction. Considering the above stated values, particle size calculated was 17.74 nm.

Green synthesis of ZnO NPs was performed using flower extract of *Nyctanthes arbor-tristis* and sizes deciphered for green [29] and chemical ZnO NPs are summarized in Table 2. Characterization techniques confer little variation between ZnO NPs obtained by the two methods of synthesis. The particles had similar sizes and polydispersity indices, which emphasize that mode of synthesis, had little effect on the resultant nanopowder.

Antimicrobial potential of nanoparticle impregnated with fungicides

Nanoparticles possess good antimicrobial activity and though the exact mechanism of action is not known, a range of effectors are supposedly involved in microbial inhibition mediated by NPs. Apparently, disruption of membrane structure, the release of reactive oxygen species and hydrogen peroxide are mainly involved in the antimicrobial potential of ZnO NPs [39-41]. Chemically synthesized ZnO NPs showed good antifungal activity against tested fungal phytopathogens (Fig. 5). MIC values of green [29] and chemical ZnO NPs were determined and results are presented in Table 3.

MIC values of ZnO NPs against test fungi ranged between 16- 128 µg/mL and results obtained were found to be in accordance with reports available. Commercially available ZnO NPs with the size of 70 ± 15 nm were found to significantly inhibit the growth of *B. cinerea* and *P. expansum* at concentrations greater than 3 mmol/L (approximately, 244 µg/mL). Further, *P. expansum* was found to be more sensitive than *B. cinerea* [42]. In the current study, however, both the fungi were found to be equally susceptible to MIC value of 128 µg/mL. Also, MIC value of 16 µg/mL was observed for A. niger, very similar to that reported by Singh and Nanda (12.5 µg/mL) [43]. Mycelial growth of *Rhizoctonia solani* and *Sclerotinia homoeocarpa*

Table 1: d-spacing calculations for ZnO NPs.

Peak 2θ	θ	$\sin\theta$	$d = n\lambda / 2\sin\theta$ (Å)	d (nm)	*hkl*
31.86	15.93	0.274	2.811	0.2811	100
34.52	17.26	0.297	2.594	0.2594	002
36.34	18.17	0.312	2.469	0.2469	101
47.56	23.78	0.403	1.911	0.1911	102
56.74	28.37	0.475	1.622	0.1622	110
62.96	31.48	0.522	1.476	0.1476	103
66.46	33.23	0.548	1.406	0.1406	200
67.98	33.99	0.559	1.378	0.1378	112
69.14	34.57	0.567	1.359	0.1359	201

Table 2: Size of Nanoparticles Deciphered by Various Analytical Techniques.

Nanoparticle	Size (nm) calculation based on			Polydispersity Index
	TEM	XRD	DLS	
Green ZnO NP	12-32	16.76	74.36	0.488
Chemical ZnO NP	12-63	17.74	76.15	0.493

Table 3: MIC values of chemical ZnO NPs and green ZnO NPs.

Fungus	MIC (µg/mL)	
	Green ZnO NP	Chemical ZnO NP
A. alternata	64	64
A. niger	16	16
B. cinerea	128	128
F. oxysporum	64	64
P. expansum	128	128

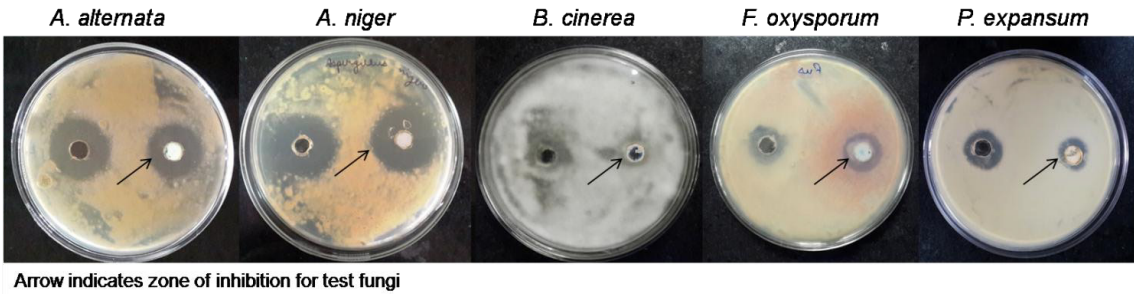

Fig. 5: Inhibition of fungal phytopathogens by ZnO NPs.

were found to be substantially inhibited at ZnO NP concentrations of 100 µg/mL and ≥ 200 µg/mL, respectively [44, 45]. These reports indicate an excellent antimicrobial potential of ZnO NPs. Since, the antimicrobial potential of NPs showed a correlation with size, shape and concentration [46]; analogous MIC values could be attributed to similar shape and size range of NPs obtained by both green and chemical methods with no effect of synthesis pathway adopted.

Further, efforts were made to study the effect of NPs in combination with three commonly used fungicides, viz., carbendazim, mancozeb and thiram. MIC values of fungicides individually were also investigated for reaching to a comparative analysis. Carbendazim is a broad spectrum systemic fungicide and apparently suppresses the assembly of β-tubulin during mitosis, arresting the cell cycle in mitotic phase and inhibits cell division [47]. Mancozeb and thiram, on the other hand, have contact based action. Mancozeb has a multi site activity and can be metabolized to yield its N-nitroso compounds, which act as alkylating agents and can react with cellular molecules such as DNA and proteins, interfering with normal metabolic processes [48]. It is further known to interfere with lipid metabolism of target cells [49]. Thiram is multi-use carbamate fungicide and is used as a protective fungicide and mammal repellant. While bad taste is responsible for repellant properties; fungicidal action is mediated by inhibition of mycelia growth, spore germination [50] and inactivation of glutathione reductase [51]. Of the three, carbendazim was found to be most effective with MIC value of 1 µg/mL for *A. niger* and *B. cinerea* and 2 µg/mL for *A. alternata, F. oxysporum* and *P. expansum*. Combination activity of fungicides and ZnO NPs was evaluated against fungal phytopathogens and MIC values of fungicides were taken as comparison controls (Table 4, 5, 6). In all the experiments, MIC value was found to decrease by at least one dilution and the effect was more pronounced with NP combinations of mancozeb and thiram as compared to carbendazim. *P. expansum* was the most sensitive fungus to all tested combinations and exhibited drastic decrease in MIC values from 2 µg/mL for carbendazim alone to 0.25 µg/mL with CGZ and 4 µg/mL for thiram alone to 0.25 µg/mL for TGZ. It was followed by *A. alternata* and *A. niger* which showed a decrease from 2 and 4 µg/mL for thiram alone to 0.5 µg/mL with TGZ. Paired sample t-test analysis was performed which indicated a significant difference in the means of all the combination samples with respect to individual fungicides. The t- statistic values ranged from 4.1 to 5.3, higher than the p-value of 2.78 at the significance level of 0.05 and degree of freedom = 4.

When comparing among the three tested fungicides, it was clearly evident that sulfur-containing mancozeb and thiram offer better results. Xue *et al.* have reported an interaction between ZnO NPs and thiram via the S atoms in the latter, to yield a composite system. It is given that sulfur atoms in thiram have a higher affinity for zinc atoms as compared to oxygen and facilitates the replacement of adsorbed water molecules with thiram, resulting in a stable composite of ZnO NPs with the fungicide [52]. The similar interaction could be involved in the composite system of ZnO NPs with mancozeb. This interaction improves the availability of both components of the composite system to the target cells, providing better inhibitions. In the given synergistic system of ZnO NPs and thiram, the authors have also shown that photo-catalytic action of ZnO NPs led to complete degradation of thiram under sunlight [52]. This provides an added advantage of using the suggested combination,

Table 4: Effect of nanoparticles on the efficacy of carbendazim.

Fungus	Carbendazim	CGZ	CCZ
A. alternata	2	1	1
A. niger	1	0.5	0.5
B. cinerea	1	0.5	0.5
F. oxysporum	2	0.5	0.5
P. expansum	2	0.25	0.5
Mean	1.6	0.55	0.6
sd	0.55	0.27	0.22
SEM	0.25	0.12	0.10
t value		4.12	4.47
Inference		Significant	Significant

Table 5: Effect of nanoparticles on the efficacy of mancozeb.

Fungus	Mancozeb	MGZ (Green)	MCZ (Chemical)
A. alternata	4	1	1
A. niger	8	1	2
B. cinerea	8	2	4
F. oxysporum	4	2	2
P. expansum	4	0.5	1
Mean	5.6	1.3	2
sd	2.19	0.67	1.22
SEM	0.98	0.30	0.55
t value		4.56	5.31
Inference		Significant	Significant

where not only the fungicidal activity is enhanced but the degradation of fungicide without any additional efforts proves to be environmentally friendly. Similar degradation studies could also be performed for other fungicides.

Fungicidal action coupled with oxidative damage by ZnO NPs most likely enhanced the inhibition of fungal growth. Also, membrane disruption by ZnO NPs could be another cause of notable enhancement in their activity in combination with NPs, as it increases the penetration and internalization of the fungicide into the cells. ZnO NPs have been investigated for their antimicrobial potential individually [53-57] and also in combination with various antibiotics to study their synergistic effect [58-60]. Isaei *et al.* synthesized ZnO NPs using chemical reduction process and sputter coated them with gold. These particles were then subjected to antimicrobial studies alone and in combination with ceftazidime. It was observed that the combination at the concentration of 7 mM ZnO NPs and 32 µg/ml ceftazidime showed improved inhibition of ceftazidime-resistant *P. aeruginosa*. The effects were found to be strictly dependant on the concentration of the drug and ZnO NPs used [58]. Ghasemi and Jalal used clinical isolates of *A. baumanii* resistant to multiple drugs (ciprofloxacin,

Table 6: Effect of nanoparticles on the efficacy of thiram.

Fungus	Thiram	TGZ (Green)	TCZ (Chemical)
A. alternata	2	0.5	1
A. niger	4	0.5	1
B. cinerea	4	1	1
F. oxysporum	2	1	1
P. expansum	4	0.25	0.5
Mean	3.2	0.65	0.9
sd	1.10	0.34	0.22
SEM	0.49	0.15	0.10
t value		4.64	4.27
Inference		Significant	Significant

ceftazidime, ampicillin, amikacin, cefalotin and cloxacillin) to study inhibitory effects of ZnO NPs. ZnO NPs showed excellent inhibition of the MDR strain and also improved the antibacterial activity of ciprofloxacin and ceftazidime. Again, inhibitory effects were found to be concentration dependent and maximum inhibition was observed when 0.25 mg/mL ZnO NPs were combined with 8 µg/ml ciprofloxacin and 32 µg/ml ceftazidime. Thus, *A. baumanii* isolates otherwise resistant to both the antibiotics, showed significant inhibition when antibiotics were used in combination with ZnO NPs [59-61].

In the current study, green synthesized ZnO NPs showed better results when compared to chemically synthesized nanoparticles, possibly due to the effect of capping of phytochemicals. Green ZnO NPs were synthesized using flower extract of *Nyctanthes arbortristis*, which is a good antimicrobial in itself [61]. Since, green and chemical ZnO NPs showed similar activities individually, it is possible that overnight incubation of NPs and fungicides might have led to some positive interaction between the capping phytochemicals and the fungicides which, in turn, further improved the overlay of fungicides onto the surface of green ZnO NPs and hence, activity of given combination.

CONCLUSION

The current study reports synthesis and characterization of ZnO NPs using UV-Vis spectroscopy, XRD, DLS and TEM. The nanopowder obtained was in polydisperse form and had an average hydrodynamic diameter of 76.15 nm, while individual particle size was found to be 17.74 nm. The nanopowder was effective against fungal phytopathogens and inhibitory effects were found to be size and concentration dependent. When used in combination with fungicides, NPs enhanced their activity. Use of fungicides has always been the method of choice when it comes to warding off fungal infections. However, synthetic chemical fungicides not only prove toxic to the environment but are also rendered ineffective by target fungi, by developing resistance mechanisms to evade their inhibitory effects over time. This has led the farmers to use even higher concentrations of fungicides for successful protection, further exaggerating their toxic effects and ingression in the food chain. ZnO NPs, on the other hand, are biocompatible and exert microbial inhibition by an array of mechanisms, making it unlikely for microorganisms to develop complete resistance against them. Combination of fungicides and ZnO NPs will not only be effective against fungal pathogens in smaller concentration and less prone to development of resistance; but also, ZnO mediated degradation of fungicides could provide for a remediation technique for removal of fungicides form the environment. It could be concluded that currently reported combinations have the potential to act as environment friendly formulation in the fight against plant fungal infections, though extensive studies about all involved interactions, persistence and effect of NPs in the environment need to be conducted.

ACKNOWLEDGEMENT

The author PJ is thankful for Assured Opportunity for Research Careers (AORC), Department of Science and Technology (DST), Ministry of Science and Technology, New Delhi for awarding INSPIRE fellowship. All the authors are thankful to Sophisticated Analytical Instrument Facility (SAIF), AIIMS, New Delhi for providing TEM facility and Indian Agricultural Research Institute (IARI), New Delhi for the supply of fungal cultures.

CONFLICT OF INTEREST

On behalf of all authors, the corresponding author states that there is no conflict of interest.

REFERENCES

[1] Grover A., Gowthaman R., (2003), Strategies for development of fungus-resistant transgenic plants. *Curr. Sci. India.* 84: 330-340.

[2] Pennisi E., (2001), The push to pit genomics against fungal pathogens. *Science.* 292: 2273-2274.

[3] IANS-Indo-Asian News Service, (2012), Stop fungal disease in crops, feed 600 million. http://zeenews.india.com/news/eco-news/stop-fungal-disease-in-crops-feed-600-million_769673.html. Published 12 April 2012, Accessed 9 January 2015.

[4] Liu J., Sui Y., Wisniewski M., Droby S., Liu Y., (2013), Review: Utilization of antagonistic yeasts to manage postharvest fungal diseases of fruit. *Int. J. Food Microbiol.* 167: 153-160.

[5] Leroch M., Kretschmer M., Hahn M., (2011), Fungicide resistance phenotypes of *Botrytis cinerea* isolates from commercial vineyards in South West Germany. *J. Phytopathol*. 159: 63–65.

[6] Jamdagni P., Rana J. S., Khatri P., (2017), Rapid optical detection strategy for human pathogens: A brief review. *J. Infect. Dis. Diagn.* 2: 115-121.

[7] Khatami M., Amini E., Amini A., Mortazavi S. M., Farahani Z. K., Heli H., (2017), Biosynthesis of silver nanoparticles using pine pollen and evaluation of the antifungal efficiency. *Iranian J. Biotech.* 15: 95-101.

[8] Khatami M., Heli H., Jahani P. M., Azizi H., Nobre M. A. L., (2017), Copper/copper oxide nanoparticles synthesis using *Stachys lavandulifolia* and its antibacterial activity. *IET Nanobiotechnol*. 11: 709-713.

[9] Khatami M., Kharazi S., Farahani Z. K., Azizi H., Nobre M. A. L., (2017), The anti-cancer effect of octagon and spherical silver nanoparticles on MCF-7 breast cancer cell line. *Tehran Univ. Med. J*. 75: 72-76.

[10] Ahmed S., Ahmad M., Swami B. L., Ikram S., (2016), A review on plants extract mediated synthesis of silver nanoparticles for antimicrobial applications: A green expertise. *J. Adv. Res.* 7: 17–28.

[11] Azizi Z., Pourseyedi S., Khatami M., Mohammadi H., (2016), S*tachys lavandulifolia* and *Lathyrus sp.* mediated for green synthesis of silver nanoparticles and evaluation its antifungal activity against *Dothiorella sarmentorum. J. Clust. Sci.* 27: 1613-1628.

[12] Bobo D., Robinson K. J., Islam J., Thurecht K. J., Corrie S. R., (2016), Nanoparticle-based medicines: A review of FDA-approved materials and clinical trials to date. *Pharm. Res.* 33: 2373–2387.

[13] Chen G., Roy I., Yang C., Prasad P. N., (2016), Nanochemistry and nanomedicine for nanoparticle-based diagnostics and therapy. *Chem. Rev.* 116: 2826–2885.

[14] Jamdagni P., Khatri P., Rana J. S., (2016), Nanoparticles based DNA conjugates for detection of pathogenic microorganisms. *Int. Nano Lett.* 6: 139-146.

[15] Khatami M., Nejad M. S., Salari S., Almani P. G. N., (2016), Plant-mediated green synthesis of silver nanoparticles using *Trifolium resupinatum* seed exudate and their antifungal efficacy on *Neofusicoccum parvum* and *Rhizoctonia solani*. *IET Nanobiotechnol.* 10: 237-243.

[16] Nejad M. S., Bonjar G. H. S., Khatami M., Amini A., Aghighi S., (2017), *In vitro* and *in vivo* antifungal properties of silver nanoparticles against *Rhizoctonia solani*, a common agent of rice sheath blight disease. *IET Nanobiotechnol*. 11: 236-240.

[17] Sirelkhatim A., Mahmud S., Seeni A., Kaus N. H. M., Ann L. C., Bakhori S. K. M., Hasan H., Mohamad D., (2015), Review on zinc oxide nanoparticles: Antibacterial activity and toxicity mechanism. *Nano-Micro Lett.* 7: 219–242.

[18] Food and Drug Administration, (2015), Select Committee on GRAS Substances Opinion: Zinc Salts. USA. http://www.fda.gov/Food/IngredientsPackagingLabeling/GRAS/SCOGS/ucm261041.htm. Accessed 25 August 2016.

[19] Espitia P. J. P., Soares N. F. F., Coimbra J. S. R., de Andrade N. J., Cruz R. S., Medeiros E. A. A., (2012), Zinc oxide nanoparticles: Synthesis, antimicrobial activity and food packaging applications. *Food Bioproc. Technol*. 5: 1447–1464.

[20] Li Q., Mahendra S., Lyon D. Y., Brunet L., Liga M. V., Li D., Alvarez P. J., (2008), Antimicrobial nanomaterials for water disinfection and microbial control: potential applications and implications. *Water Res*. 42: 4591-4602.

[21] Marcous A., Rasouli S., Ardestani F., (2017), Low-density polyethylene films loaded by titanium dioxide and zinc oxide nanoparticles as a new active packaging system against *Escherichia coli* O157:H7 in fresh calf minced meat. *Packag. Technol. Sci*. 30: 693-701.

[22] Marcous A., Rasouli S., Ardestani F., (2017), Inhibition of *Staphylococcus aureus* growth in fresh calf minced meat using low density polyethylene films package promoted by titanium dioxide and zinc oxide nanoparticles. *J. Partic. Sci. Technol.* 3: 1-11.

[23] Güy N., Özacar M., (2016), The influence of noble metals on photocatalytic activity of ZnO for congo red degradation. *Int. J. Hydrogen Energy.* 41: 20100-20112.

[24] Rokhsat E., Akhavan O., (2016), Improving the photocatalytic activity of graphene oxide/ZnO nanorod films by UV irradiation. *Appl. Surf. Sci.* 371: 590-595.

[25] Soltaninezhad M., Aminifar A., (2011), Study nanostructures of semiconductor zinc oxide (ZnO) as a photocatalyst for the degradation of organic pollutants. *Int. J. Nano Dimens.* 2: 137-145.

[26] Kumar R., Umar A., Kumar G., Nalwad H. S., (2017), Antimicrobial properties of ZnO nanomaterials: A review. *Ceram. Int.* 43: 3940-3961.

[27] Narasimha G., Sridevi A., Prasad B. D., Kumar B. P., (2014), Chemical synthesis of zinc oxide (ZnO) nanoparticles and their antibacterial activity against a clinical isolate *Staphylococcus aureus. Int. J. Nano Dimens.* 5: 337-340.

[28] Central Insecticides Board & Registration Committee, (2017), Ministry of Agriculture & Farmers Welfare, India. http://cibrc.nic.in/. Accessed 28 June 2017.

[29] Jamdagni P., Khatri P., Rana J. S., (2016), Green synthesis of

zinc oxide nanoparticles using flower extract of *Nyctanthes arbor-tristis* and their antifungal activity. *J. King Saud. Univ., Sci*. doi:10.1016/j.jksus.2016.10.002.

[30] Gnanasangeetha D., Thambavani S., (2013), One pot synthesis of zinc oxide nanoparticles via chemical and green method. *Res. J. Mater. Sci*. 1: 1-8.

[31] Jayaseelan C., Rahuman A. A., Kirthi A. V., Marimuthu S., Santhoshkumar T., Bagavan A., Gaurav K., Karthik L., Rao K. V., (2012), Novel microbial route to synthesize ZnO nanoparticles using *Aeromonas hydrophila* and their activity against pathogenic bacteria and fungi. *Spec. Chimi. Acta A. Mol. Biomol. Spec.* 90: 78-84.

[32] Tantra R., Schulze P., Quincey P., (2010), Effect of nanoparticle concentration on zeta-potential measurement results and reproducibility. *Particuology.* 8: 279–285.

[33] Jamdagni P., Khatri P., Rana J. S., (2018), Biogenic synthesis of silver nanoparticles from leaf extract of *Elettaria cardamomum* and their antifungal activity against phytopathogens. *Adv. Mater. Proc.* 3: 129–135.

[34] Yung K., Ming H., Yen C., Chao H., (2012), Synthesis of 1D, 2D and 3D ZnO polycrystalline nanostructures using sol-gel method. *J. Nanotechnol*. 2012: 712850-712858.

[35] Khatami M., Mehnipor R., Poor M. H. S., Jouzani G. S., (2016), Facile biosynthesis of silver nanoparticles using *Descurainia sophia* and evaluation of their antibacterial and antifungal properties. *J. Clust. Sci.* 27: 1601-1612.

[36] Talam S., Karumuri S. R., Gunnam N., (2012), Synthesis, characterization, and spectroscopic properties of ZnO nanoparticles. *ISRN Nanotechnol*. 2012: 372505-372511.

[37] Molahasani N., Sadjadi M. S., Zare K., (2013), Correlation of morphology and luminescent properties of ZnO nano particles to different surfactants via hydrothermal method. *Int. J. Nano Dimens.* 4: 161-166.

[38] Jegan A., Ramasubbu A., Karunakaran K., Vasanthkumar S., (2012), Synthesis and characterization of zinc oxide – agar nanocomposite. *Int. J. Nano Dimens.* 2: 171-176.

[39] Lipovsky A., Nitzan Y., Gedanken A., Lubart R., (2011), Antifungal activity of ZnO nanoparticles--the role of ROS mediated cell injury. *Nanotechnol.* 22: 105101-105108.

[40] Sawai J., Shoji S., Igarashi H., Hashimoto A., Kokugan T., Shimizu M., Kojima H., (1998), Hydrogen peroxide as an antibacterial factor in zinc oxide powder slurry. *J. Ferment. Bioeng.* 86: 521–522.

[41] Sinha R., Karan R., Sinha A., Khare S. K., (2011), Interaction and nanotoxic effect of ZnO and Ag nanoparticles on mesophilic and halophilic bacterial cells. *Bioresour. Technol.* 102: 1516–1520.

[42] He L., Liu Y., Mustapha A., Lin M., (2011), Antifungal activity of zinc oxide nanoparticles against *Botrytis cinerea* and *Penicillium expansum*. *Microbiol. Res.* 166: 207-215.

[43] Singh P., Nanda A., (2013), Antimicrobial and antifungal potential of zinc oxide nanoparticles in comparison to conventional zinc oxide particles. *J. Chem. Pharm. Res*. 5: 457-463.

[44] Zare E., Pourseyedi S., Khatami M., Darezereshki E., (2017), Simple biosynthesis of zinc oxide nanoparticles using nature's source, and it's bio-activity. *J. Mol. Struct.* 1146: 96-103.

[45] Li J., Sang H., Guo H., Popko J. T., He L., White J. C., Dhankher O. P., Jung G., Xing B., (2017), Antifungal mechanisms of ZnO and Ag nanoparticles to *Sclerotinia homoeocarpa. Nanotechnol.* 28: 155101-155108.

[46] Padmavathy N., Vijayaraghavan R., (2008), Enhanced bioactivity of ZnO nanoparticles—an antimicrobial study. *Sci. Technol. Adv. Mat*. 9: 1-7.

[47] PPDB, Carbendazim. http://sitem.herts.ac.uk/aeru/ppdb/en/Reports/116.htm. Accessed 6 January 2017.

[48] Castro V. L., Tambasco A. J., Paraíba L. C., Tambasco D. D., (1999), Cytogenetic and teratological effects of mancozeb pre natal exposure on rats. *Braz. Arch. Biol. Technol.* 42: 127-134.

[49] PPDB, Mancozeb. http://sitem.herts.ac.uk/aeru/ppdb/en/Reports/424.htm. Accessed 6 January 2017.

[50] PPDB, Thiram. http://sitem.herts.ac.uk/aeru/ppdb/en/Reports/642.htm. Accessed 6 January 2017.

[51] Elskens M. T., Penninckx M. J., (1997), Thiram and dimethyldithiocarbamic acid interconversion in *Saccharomyces cerevisiae*: A possible metabolic pathway under the control of the glutathione redox cycle. *Appl. Environ. Microb*. 63: 2857–2862.

[52] Xue J., Luo Z., Li P., Ding Y., Cui Y., Wu Q., (2014), A residue-free green synergistic antifungal nanotechnology for pesticide thiram by ZnO nanoparticles. *Sci. Rep*. 4: 5408-5415.

[53] Chauhan R., Reddy A., Abraham J., (2015), Biosynthesis of silver and zinc oxide nanoparticles using *Pichia fermentans* JA2 and their antimicrobial property. *Appl. Nanosci*. 5: 63-71.

[54] Kairyte K., Kadys A., Luksiene Z., (2013), Antibacterial and antifungal activity of photoactivated ZnO nanoparticles in suspension. *J. Photochem. Photobiol*. *B*. 128: 78-84.

[55] Narendhran S., Sivaraj R., (2016), Biogenic ZnO nanoparticles synthesized using *L. aculeata* leaf extract and their antifungal activity against plant fungal pathogens. *Bull. Mater. Sci.* 39: 1-5.

[56] Rajiv P., Rajeshwari S., Venckatesh R., (2013), Bio-fabrication of zinc oxide nanoparticles using leaf extract of *Parthenium hysterophorus* L. and its size-dependent antifungal activity against plant fungal pathogens. *Spec. Chim. Acta Part A.* 112: 384–387.

[57] Sharma R. K, Ghose R., (2015), Synthesis of zinc oxide nanoparticles by homogeneous precipitation method and its application in antifungal activity against *Candida albicans*. *Ceram. Int.* 41: 967–975.

[58] Isaei E., Mansouri S., Mohammadi F., Taheritarigh S., Mohammadi Z., (2016), Novel combinations of synthesized ZnO NPs and ceftazidime: Evaluation of their activity against standards and new clinically isolated *Pseudomonas aeruginosa*. *Avicenna J. Med. Biotechnol.* 8: 169-174.

[59] Ghasemi F., Jalal R., (2016), Antimicrobial action of zinc oxide nanoparticles in combination with ciprofloxacin and ceftazidime against multidrug-resistant *Acinetobacter baumannii*. *J. Glob. Antimicrob. Resist*. 6: 118–122.

[60] Luo Z. H., Wu Q.S., Xue J. Z., Ding Y. P., (2013), Selectively enhanced antibacterial effects and ultraviolet activation of antibiotics with ZnO nanorods against *Escherichia coli*. *J. Biomed. Nanotechnol*. 9: 69–76.

[61] Khatri P., Jamdagni P., Sindhu A., Rana J. S., (2016), Antimicrobial potential of important medicinal plants of India. *Int. J. Microb. Res. Technol.* 3: 301-308.